JOURNAL OF PROPULSION AND POWER
Vol. 12, No. 3, May–June 1996

Role of Combustion on Droplet Transport in Pressure-Atomized Spray Flames

A. K. Gupta*
University of Maryland, College Park, Maryland 20742
C. Presser† and J. T. Hodges‡
National Institute of Standards and Technology, Gaithersburg, Maryland 20899
and
C. T. Avedisian§
Cornell University, Ithaca, New York 14853

The transport of droplets in a pressure-atomized kerosene spray flame was examined using a two-component phase Doppler system to measure the droplet size and velocity distributions at several locations within the spray. The effect of combustion on droplet transport was examined by comparing the results to a nonburning spray under similar flow conditions. Directions of motion of droplets are calculated from the measured droplet velocity components to provide information on trajectories and dispersion of droplets. Results show that combustion reduces the strength of gas recirculation as evidenced by significantly fewer droplets being transported upstream toward the nozzle along the centerline for the burning spray as compared to the nonburning spray. Combustion enhances droplet vaporization and results in reduced number density and larger droplet mean diameters and velocities when compared to the nonburning spray. At the spray centerline, there is a wide range of droplet trajectories that are associated with recirculated droplets and those originating from the nozzle. There is some correlation between droplet velocity and diameter. Some larger size droplets are also found to be entrained into the recirculation pattern. At the spray boundary, few droplets deviate from the mean direction. Also, droplet velocity is well correlated with increasing diameter but appears to approach an asymptotic value in which droplet velocity becomes insensitive to diameter.

I. Introduction

SPRAY flames are commonly stabilized by using swirl burners to recirculate combustion gases and fuel vapors. This class of burners has attracted considerable attention because of the potential to improve combustion efficiency and reduce pollutant emissions in the waste disposal and power generation industries. The aerothermochemistry of swirl-stabilized spray flames depends significantly on the degree of mixing between the fuel droplets and coflowing airstream. Nevertheless, most investigations on mixing and turbulence–chemistry interactions in combustion processes have dealt with gaseous-fueled flames[1] (i.e., no droplets present). Such studies can provide insights into the complex problem of droplet/air mixing, but only for very small droplets if they are assumed to follow the gas flow pattern.[2] For larger droplets that do not tend to follow the gas flow, a more complete picture of fuel transport in the spray flame is realized via spatially resolved measurements of droplet velocity.

This article examines from an experimental point of view droplet transport in a swirl-stabilized kerosene spray flame. Measurements of droplet diameter, number density, and velocity were carried out at different spatial positions using phase Doppler interferometry. These results are presented, in contrast to a recent study[3] of a kerosene spray flame in which droplet mean velocities were reported using a laser velocimetry system. Mean properties characterize the global features of a spray, whereas size and velocity distributions provide a more detailed picture of the behavior of individual droplets. In the present study, measured droplet velocity components are used to determine the direction of droplet motion throughout the spray from which conclusions are drawn concerning droplet transport. The results are compared with data for a nonburning kerosene spray[3] for the same conditions of fuel and airflow rates, and swirl, to assess the influence of combustion on droplet transport.

Data are presented at several locations in the spray. Locations are chosen where gas recirculation near the nozzle results in significant droplet dispersion (i.e., near the central region of the spray), and where the droplet concentration is relatively high (i.e., near the spray boundary). For the latter case, droplets are transported in a ballistic fashion, as their motion is not influenced strongly by the surrounding airflow pattern.

II. Experimental Apparatus

Experiments were carried out in a spray combustion facility that has been described previously.[3–6] The facility includes a swirl burner with a movable 12-vane swirl cascade (see Fig. 1). The vanes rotate simultaneously to impart the desired degree of swirl intensity (defined by the swirl number S, which is the ratio of axial fluxes of angular momentum to linear momentum)[7] to the airstream that surrounds the fuel nozzle. The value of $S = 0.53$ was chosen for the present study because it produces a stable flame stationed approximately 20 mm downstream the nozzle exit, and results can be compared to prior studies under nonburning conditions.[3] The flame structure is also characteristic of that found in many industrial combustion systems.

Presented as Paper 94-0115 at the AIAA 32nd Aerospace Sciences Meeting and Exhibit, Reno, NV, Jan. 10–13, 1994; received Feb. 7, 1994; revision received Sept. 21, 1995; accepted for publication Oct. 19, 1995.

*Professor, Department of Mechanical Engineering. Fellow AIAA.
†Leader, High Temperature Processes Group, Chemical Science and Technology Laboratory. Associate Fellow AIAA.
‡Research Engineer, Process Sensing Group, Chemical Science and Technology Laboratory.
§Professor, Department of Mechanical and Aerospace Engineering, Associate Fellow AIAA.

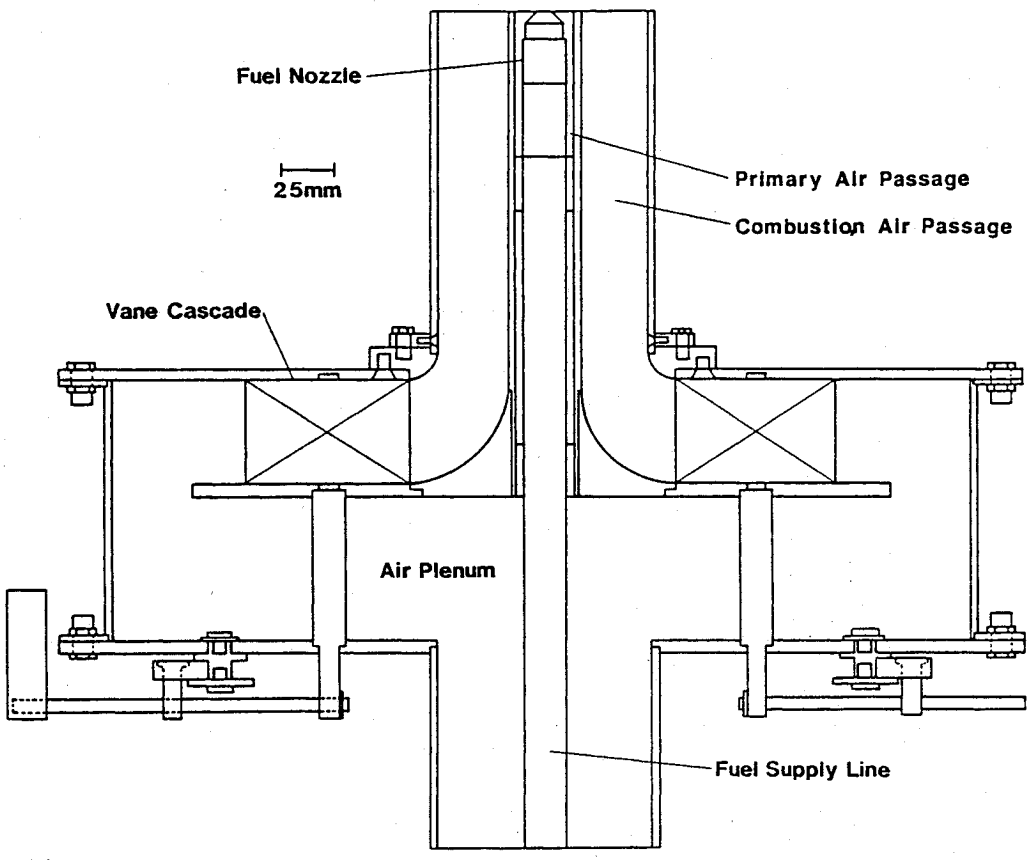

Fig. 1 Schematic of the movable-vane swirl burner.

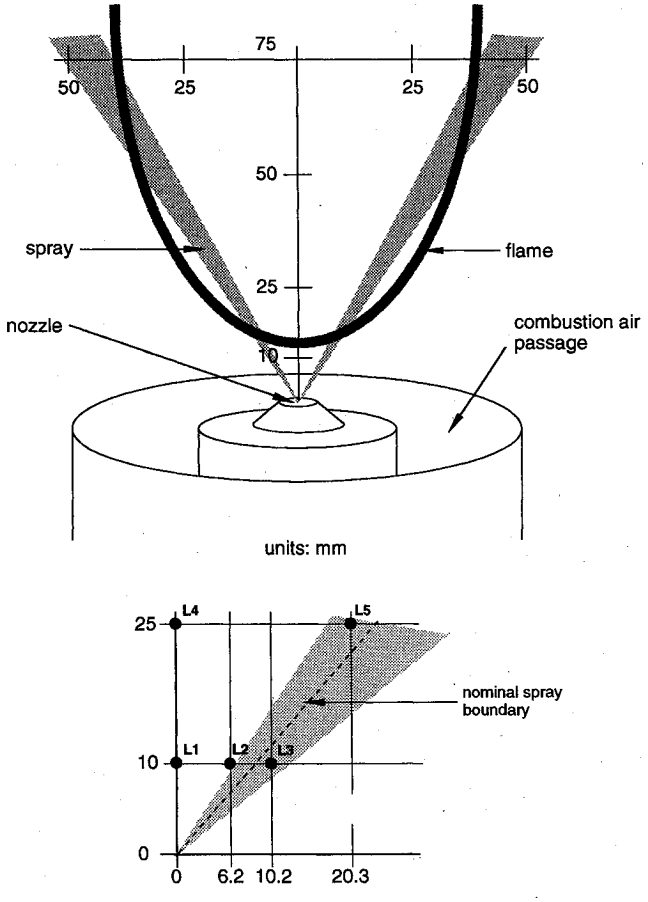

Fig. 2 Schematic of the spray boundary position relative to the flame sheet. The numbers identify particular locations where the flow parameters are discussed in detail.

A simplex pressure-jet fuel nozzle, located at the exit plane and centerline of the burner, is operated at total air and fuel flow rates of 64.3 and 3.2 kg/h, respectively; these flow rates provided an input equivalence ratio of approximately 0.75. The nozzle generates a nominal 30-deg (half angle) hollow-cone kerosene spray under unconfined conditions that is injected vertically upwards from the nozzle. A schematic of the spray relative to the flame envelope, which includes the measurement grid, is illustrated in Fig. 2. Also shown are coordinates for several specific locations (designated L1–L5) where results are discussed in more detail. Locations L1, L2, and L4 are representative of the central region of the spray where recirculation of the surrounding gases and droplet entrainment is expected to be significant. Locations L3 and L5 correspond to the spray boundary.

A stepper-motor-driven, three-dimensional traversing arrangement translates the burner assembly in the vertical and horizontal directions (see Fig. 3). All optical diagnostics are fixed in position about the burner assembly and the burner translates independently of the optical equipment. Measurements of radial profiles of the burning spray properties, e.g., droplet size, number density, velocity, etc., are carried out at different spatial positions (in radial increments of 2 mm across the burner). Enough symmetry is assumed to exist about the spray axis so that measurements of spray properties in any particular plane containing that axis are considered representative of the entire spray. Measurements are reported in the plane in which the burner is traversed (X in Fig. 3). Additional details can be found elsewhere.[3-5]

A two-channel phase Doppler interferometer[8] (PDI) was used to obtain droplet size and velocity information on individual droplets passing through the measurement volume (see Fig. 3). Mean properties were based on the statistical analysis of the measured size and velocity distributions. Several issues arise when using the PDI for such measurements in spray flames. These include the sensitivity of the measurements to the combustion gas temperature, and the influence of droplet

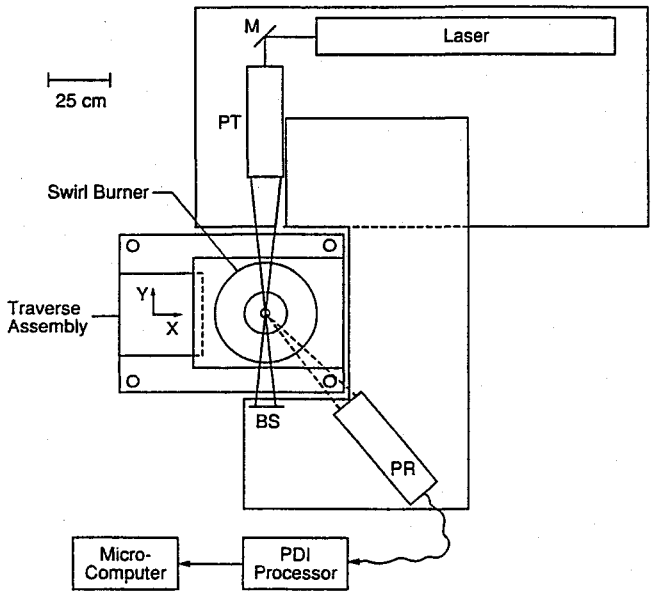

Fig. 3 Schematic of the experimental droplet size/velocity facility: BS, beam stop; PR, PDI receiving optics; PT, PDI transmitting optics; and M, mirror.

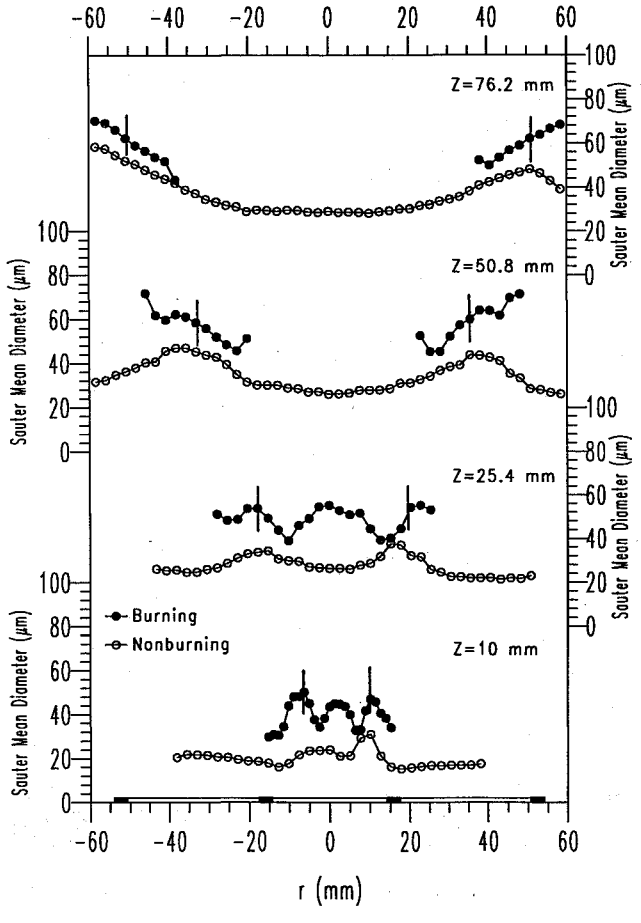

Fig. 4 Variation of D_{32} with r measured at different z for the burning and nonburning sprays.

trajectory through the probe volume on the inferred droplet size. Concerning the former, it has been demonstrated that phase Doppler measurements are insensitive to the combustion gas temperature since the technique depends weakly on droplet refractive index for nonabsorbing liquids.[9] With regard to the influence of droplet trajectory through the probe volume on inferred droplet size, such an effect can lead to the measured droplet size distribution being broader than the actual size distribution within the spray.[10] The sensitivity of measured diameter to droplet trajectory is minimized by ensuring that the characteristic width of the probe volume is much greater than the particle diameter, and by measuring the scattered light intensity in the near-forward direction.[11] In the present setup, the scattering measurements were made in the near-forward direction (30-deg scattering angle) and the minimum probe volume width was on the order of 100 μm.

The phase Doppler system provided information on particle size between 1–300 μm with the optical arrangement employed in this investigation. The measurement volume is defined by the 119- and 113-μm laser beam waists at 514.5 and 488.0 nm, respectively (with a fringe spacing of approximately 6.6 μm for both laser beams), and with the off-axis light collection optics positioned at a scattering angle of 30 deg. The focal lengths of the transmitting and receiving optics were 495 and 500 mm, respectively. The focal length of the collimating lens was 300 mm. For the experiments carried out in this investigation, the photomultiplier detector voltages were optimized to provide the greatest sensitivity to the wide range of droplet sizes typically found in these sprays. Near the spray boundary, which is defined as the location where the measured number density is largest, data acquisition rates were high (10,000 data points were collected within 120 s). However, in other regions of the spray, considerably more time was required to collect the data.

Near the spray boundary, the required system gain was significantly lower and the fraction of validated data was two to three times larger than near the spray centerline (reaching a maximum validation rate of approximately 80%). Compared to the nonburning case for which validation rates were reported at 95% near the spray boundary, in the burning spray validation rates were much lower. This reduction in validation rate is attributed to reduced signal quality. The variation in vali-

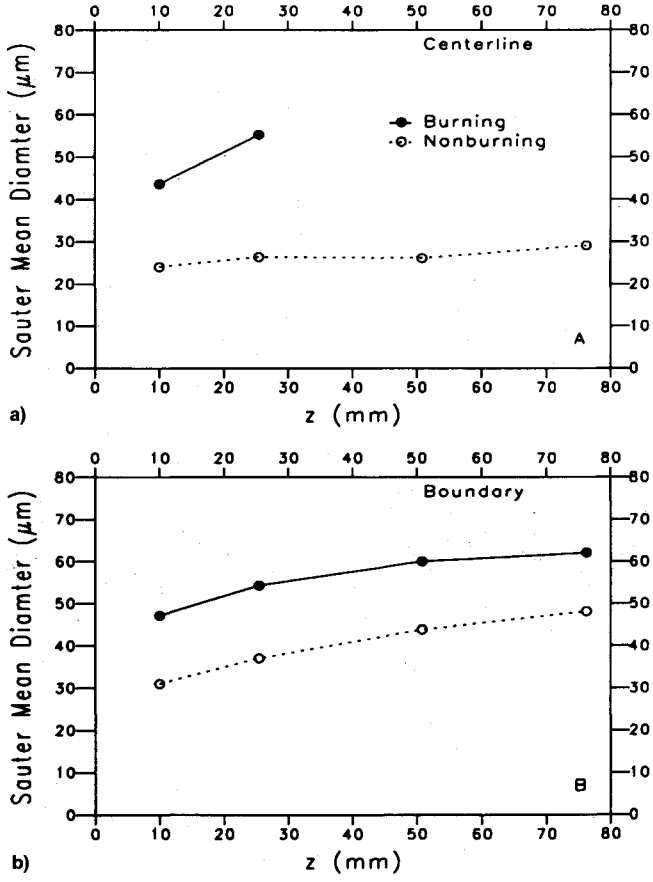

Fig. 5 Variation of D_{32} with z measured a) along the centerline and b) nominal spray boundary for the burning and nonburning sprays.

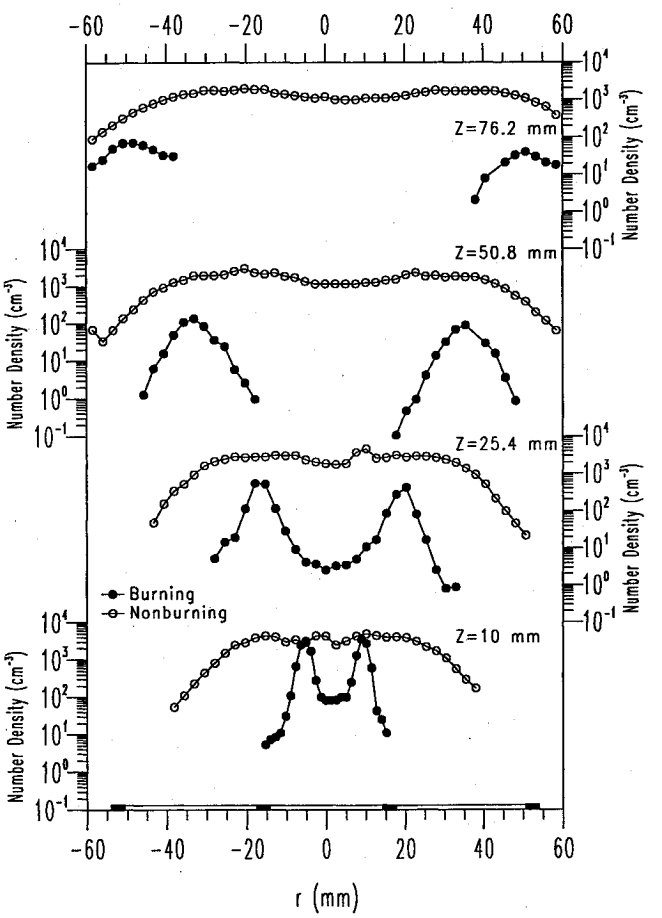

Fig. 6 Variation of N with r measured at different z for the burning and nonburning sprays.

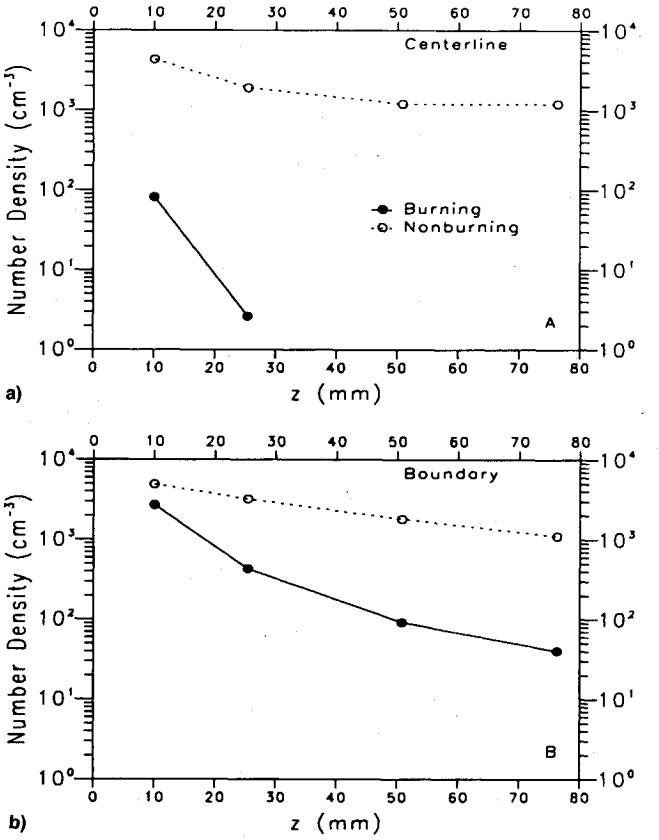

Fig. 7 Variation of N with z measured a) along the centerline and b) nominal spray boundary for the burning and nonburning sprays.

dation rate with spatial position, and its effect on number density and mass flux, is discussed in more detail elsewhere.[12,13] Measurements were repeated at several selected positions to ensure measurement repeatability that was generally better than 5% near the spray boundary.

III. Results and Discussion

A. Droplet Mean Properties

Droplet mean properties (i.e., size, number density, and velocity) are presented to describe the global features of the spray flame. The effects of combustion on droplet transport are emphasized by comparing the same spray under burning and nonburning conditions. The results for the nonburning case were taken from an earlier investigation.[5] Radial profiles of the droplet Sauter mean diameter (D_{32}) at four axial locations (z = 10, 25.4, 50.8, and 76.2 mm) downstream of the nozzle exit are presented in Fig. 4. Two cases are compared, namely, data for a burning and nonburning kerosene spray. The solid boxes along the abscissa indicate the position of the burner passage walls, with the fuel nozzle located at the axis of the burner (r = 0). The vertical bars identify the nominal spray boundary, which is defined as the radial location (at a given axial position), where the radial profiles of number density exhibit a peak (i.e., see Fig. 5). These peaks also correspond to those for volume flux (i.e., volume of the droplets passing a unit cross-sectional area per unit of time).

The central peak of D_{32} for the burning spray at z = 10 and 25.4 mm is attributed to vaporization and depletion of the smaller droplets that result in an increase in mean diameter. For the nonburning case, no central peak exists. Also, this result may be attributed, in part, to the fact that swirl exerts a greater influence on droplet mixing for a nonburning spray than a burning spray.[5] Further downstream, at z = 50.8 and

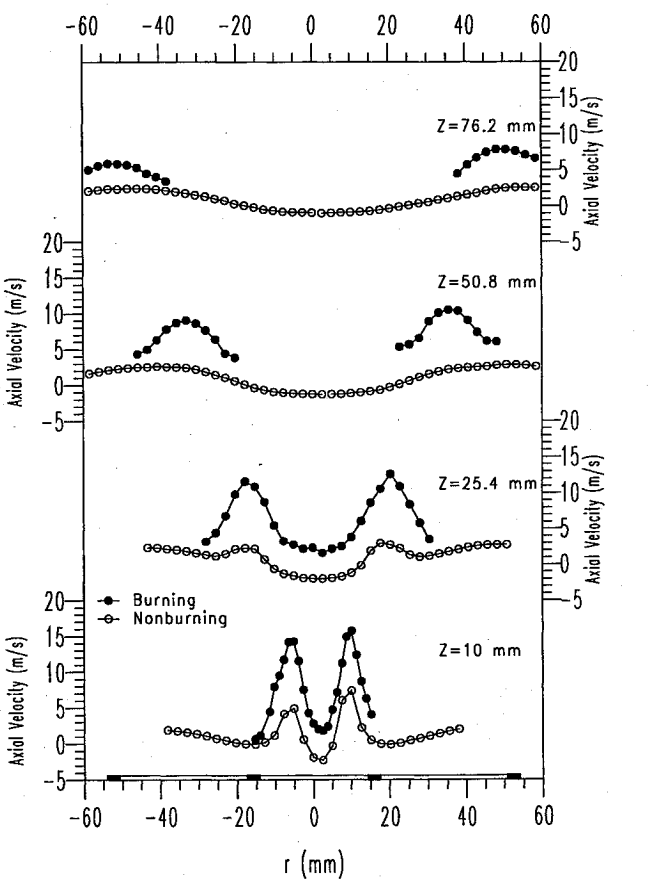

Fig. 8 Variation of u with r measured at different z for the burning and nonburning sprays.

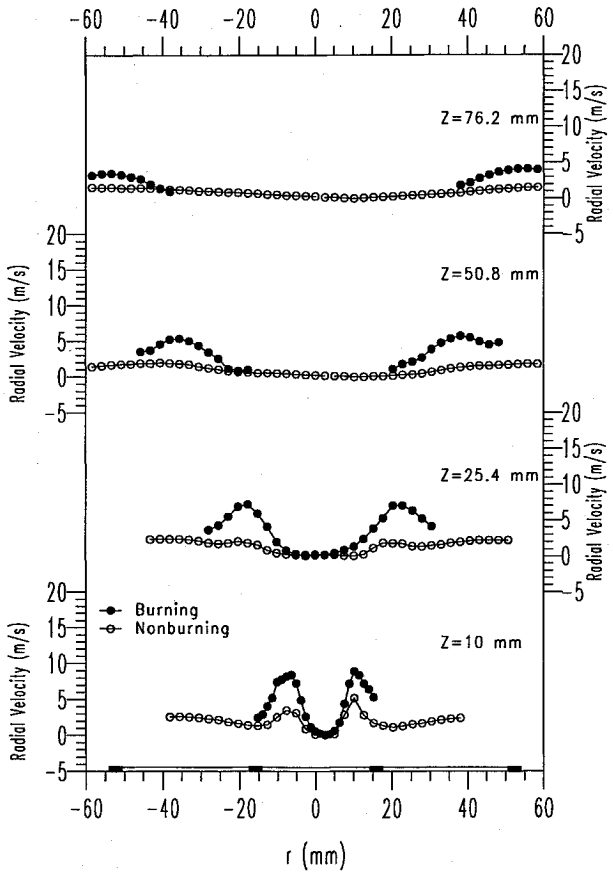

Fig. 9 Variation of v with r measured at different z for the burning and nonburning sprays.

76.2 mm, data are not reported in the center for the burning spray because of the absence of droplets at these positions. The absence of droplets at these downstream positions, compared to the relative abundance of droplets at these same locations for the nonburning spray, is indicative of the significant enhancement of heat transport and droplet vaporization associated with the high-temperature combustion gases.

The variation of droplet mean size with axial position along the centerline and spray boundary is shown in Figs. 5a and 5b, respectively. Data along the burner axis are limited for the burning case because of the aforementioned difficulties in detecting the presence of droplets at positions far downstream of the nozzle. The trends show that the values of D_{32} increase for both positions. This fact emphasizes the importance of vaporization of smaller droplets which, essentially, removes them from statistical consideration in determining mean spray properties. In addition to vaporization, other mechanisms for depletion of smaller droplets in the spray boundary include coalescence between droplets (which, however, is not expected to be significant because of the low probability of collisions between small droplets) and/or dispersion. Note that comparison of droplet size at different spatial positions, in fact, represents a different population of droplets. It is also recognized that the data obtained in this study cannot with certainty identify the precise mechanisms.

The spatial variation of droplet number density N at the four previously mentioned axial positions is shown in Fig. 6 along with data for the nonburning spray.[5] Differences among the two sets of data are substantial and illustrate the effects of combustion. The number density exhibits a peak that is reasonably symmetric around the centerline for the burning spray, whereas no such peak exists for the nonburning spray. For the nonburning spray, the values of N are essentially constant across the spray and decrease outside of the spray boundary. A close comparison of the results shown in Figs. 4 and 6 reveals that the largest droplet mean sizes reside at approximately the same radial position at which number density exhibits a peak. This result indicates that the bulk of the fuel mass resides along the spray boundary (as is characteristic of hollow-cone sprays). Determination of the volume flux also supports this conclusion.

The variation of number density with axial position is presented in Fig. 7 along both the centerline and spray boundary. The number density decreases as axial position increases for

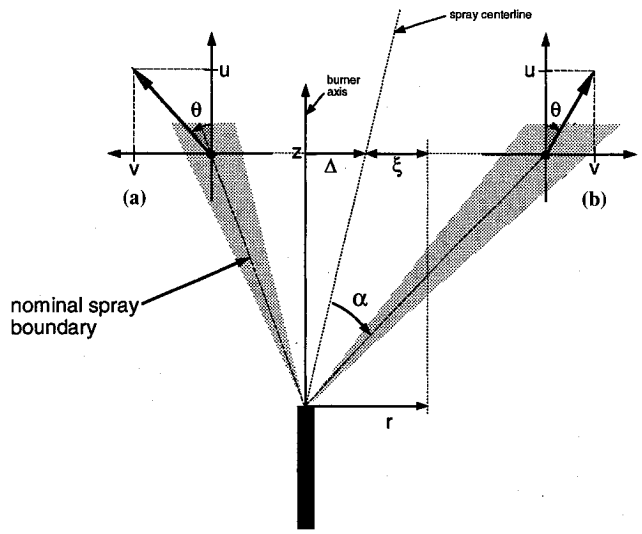

Fig. 10 Coordinate system used in the definition of θ. Coordinate (a) is replaced by (b) at the radial location where the magnitude of radial velocity component is a minimum ($\Delta = 0$ for a perfectly symmetric spray).

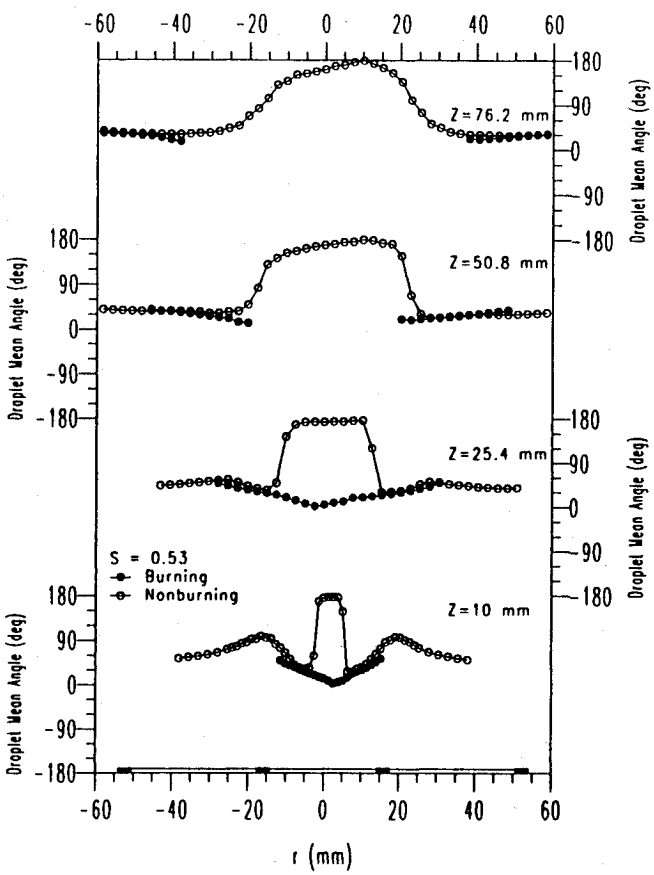

Fig. 11 Variation of θ (see Fig. 10), with r at different z for the burning and nonburning sprays.

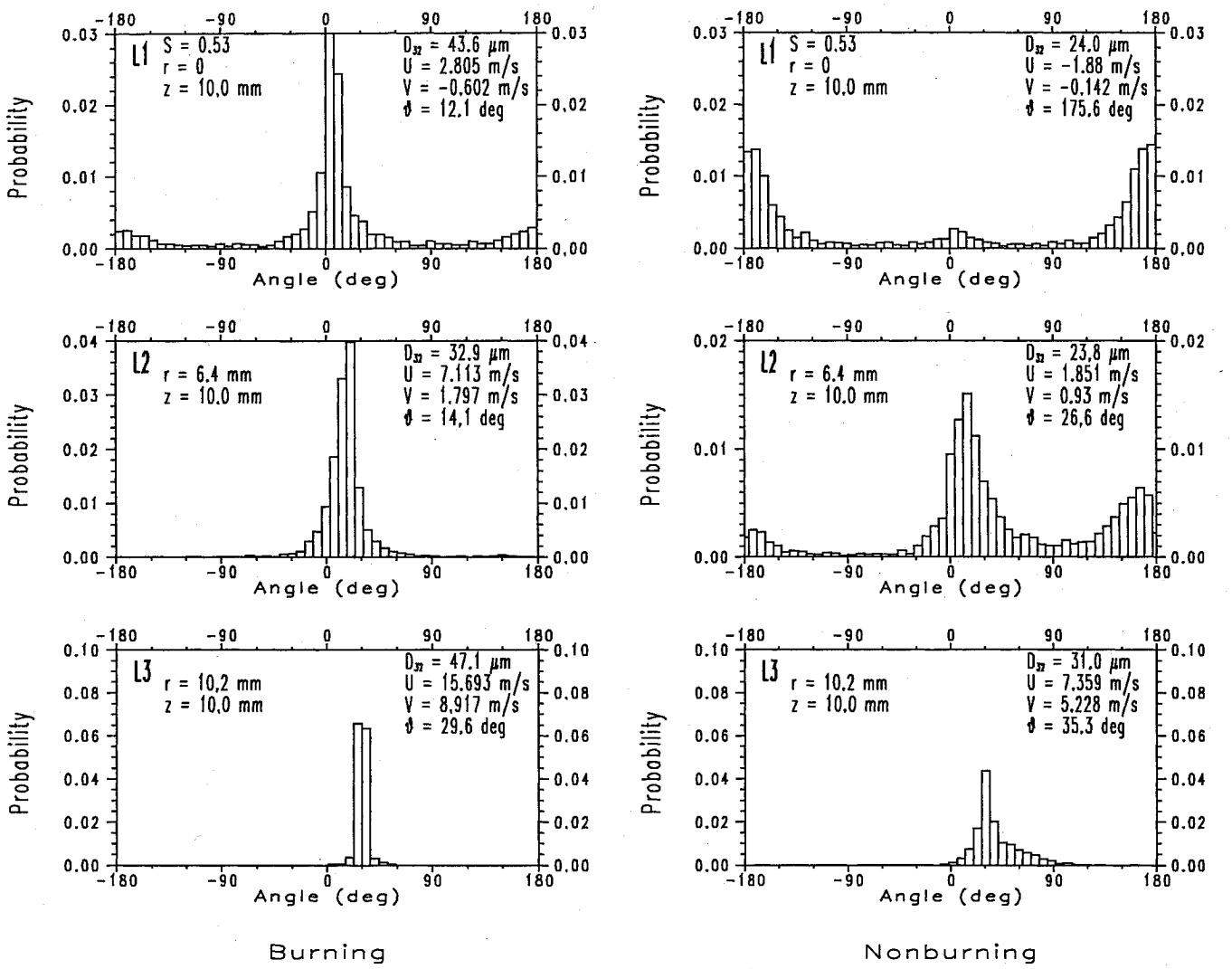

Fig. 12 Probability distributions for droplet trajectory angles at three different locations (L1–L3) in the burning and nonburning sprays for all droplet sizes.

both cases, and the values of N are larger for the nonburning spray. For example, near the spray boundary for the burning spray, number density changes by a factor of 100, i.e., from $N \approx 3 \times 10^3$ particles/cm^3 (volume flux of approximately 1×10^{-1} cm^3/s/cm^2) at $z = 10$ mm to $N \approx 4 \times 10^1$ particles/cm^3 (volume flux of approximately 3×10^{-3} cm^3/s/cm^2) at $z = 76.2$ mm. Differences among the two conditions (burning and nonburning) are the result of significant droplet vaporization, due to heat transport from the surrounding combustion gases, which deplete the population of droplets.

The spatial profiles of droplet mean axial u and radial v velocity components at the four aforementioned axial locations were measured and the results are shown in Figs. 8 and 9, respectively. Results for the burning spray are again compared with those for the nonburning spray.[5] Positive values of u correspond to droplets moving in the downstream direction (away from the atomizer) and positive values of v signify radially outward motion (negative values of v refer to droplet motion toward the centerline of the spray). Figure 8 shows that the droplet mean axial velocity decreases with increasing axial position for both the burning and nonburning sprays. In contrast to the nonburning spray, droplets in the burning spray have positive axial velocities and negligible radial velocities at positions near the axis of the burner.

The droplet axial and radial velocity components for the burning spray exhibit maxima near the spray boundary (see Figs. 8 and 9), with the mean flow corresponding to a direction that is consistent with the nominal spray cone half angle (α in Fig. 10). For example, given the peak values of $u \approx 13$ m/s and $v \approx 8$ m/s at $z = 25.4$ mm (as shown in Figs. 8 and 9), the mean flow direction θ of the droplets (see Fig. 10) is approximately 32 deg, whereas the nominal spray angle α (as specified by the nozzle manufacturer) is about 30 deg. Near the spray boundary, the values of u and v for the burning spray are at least a factor of 3 higher than those of the nonburning spray (see Figs. 8 and 9). Assuming that the droplet velocities at the nozzle are the same for both cases, this result suggests that combustion decreases significantly the mean rate of droplet deceleration.

B. Direction of Droplet Motion

The entrainment of droplets by the surrounding gaseous medium, and secondary breakup of droplets in a spray flame, are complicated phenomena involving aerodynamic drag forces and the creation of waves at the surface of droplets. Somewhat simplistic measures of these phenomena are provided by the Weber number ($=\bar{V}_{rel}^2 \rho D/\sigma$) for droplet breakup, the Stokes number ($=\rho_l D^2 \bar{V}_{rel}/18\mu\delta$) for dispersion and entrainment, and the Reynolds number ($=\bar{V}_{rel} D\rho/\mu$) for drag and internal circulation within droplets. In the definition of these parameters, $\bar{V}_{rel}$ is the relative velocity between the droplet and surrounding gas, ρ is the gas density, ρ_l is the liquid density, D is the droplet diameter, σ is the droplet surface tension, μ is the gas phase viscosity, and δ is a length scale characteristic of a vortex or eddy in the coflowing swirling gas stream. Two practical difficulties arise when evaluating these parameters for spray

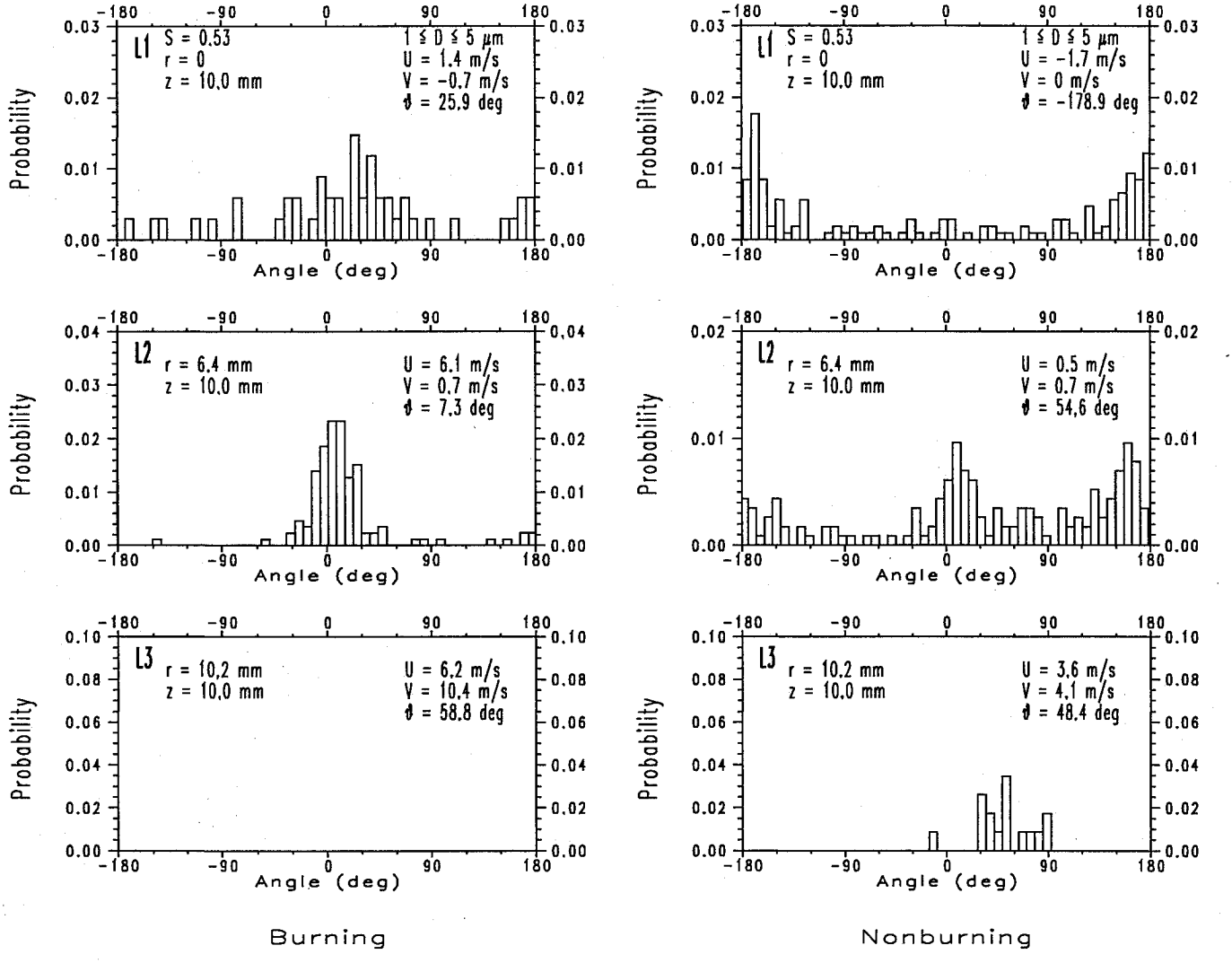

Fig. 13 Probability distributions for droplet trajectory angles at three different locations (L1–L3) in the burning and nonburning sprays for droplets in the size range of 1–5 μm.

flames. First, the droplet velocity relative to the surrounding gas phase is not easily obtained, and second, the characteristic length scale for the recirculating vortex in the definition of the Stokes number is essentially unknown.

A complete mapping of the gas phase velocity (as distinguished from the velocity of droplets) in a spray flame is complicated by the fact that typical sizes of seed particles (<5 μm) can be the same as the diameter of the smallest droplets produced by the atomization process. This fact leads to difficulties in discrimination of phases in the light scattering signal. It is difficult to distinguish between light scattering from seed particles and light scattered by liquid droplets[14,15] with current optical techniques. Attempts to bias the laser light detectors for seed particle sizes have met with limited success in dense regions of sprays because of the presence of droplets of the same size as the seed particles.[16] Of course, if it is known that droplets will not be present with diameters similar to seed particle sizes, then seed particles introduced into the flow can provide a measure of the gas phase velocity. However, this is not the case for the current conditions where significant numbers of droplets less than 5 μm are present, especially upstream near the nozzle. For this situation the small droplets (now playing the role of seed particles) must also be assumed to follow the gas flow pattern. The validity of this assumption depends on the extent to which the droplets have completely decelerated to the gas motion. Indeed, it is unlikely to be true, in general, near the nozzle because of the momentum imparted to the liquid by the forced flow of fuel through the atomizer. For these reasons, the droplet relative velocity could not be determined with certainty under the conditions examined and instrumentation used in this investigation. Therefore, it would be inappropriate to evaluate the Weber, Reynolds, and Stokes numbers. However, information related to droplet transport can still be obtained indirectly from the droplet velocity components.

The droplet velocity components were used to obtain a direction of droplet motion θ, which is defined in Fig. 10. The symbol Δ is a measure of the asymmetry of the spray. The spray centerline is therefore defined to correspond to the radial position (at any axial location) where the radial velocity component is a minimum (see convention, defined earlier, for the velocity components). When $\Delta = 0$, the spray is symmetric about the axis of the atomizer. The value of Δ is determined at any axial location by first identifying the radial location at which the radial velocity component reaches a minimum. The symbol ξ is referenced to that location and $\xi = 0$ is the centerline. For $\xi > 0$, coordinate system (b) is used, and for $\xi < 0$ coordinate system (a) is used. With this choice of an axisymmetric coordinate system and sign convention for velocity components mentioned previously, negative values of θ will correspond to velocity vectors that are directed inward toward the centerline.

In a swirl-stabilized spray, the flowfield is nominally three-dimensional and, hence, three components of the velocity vector (axial, radial, and tangential components) should be used to determine the direction of droplet motion. However, for the

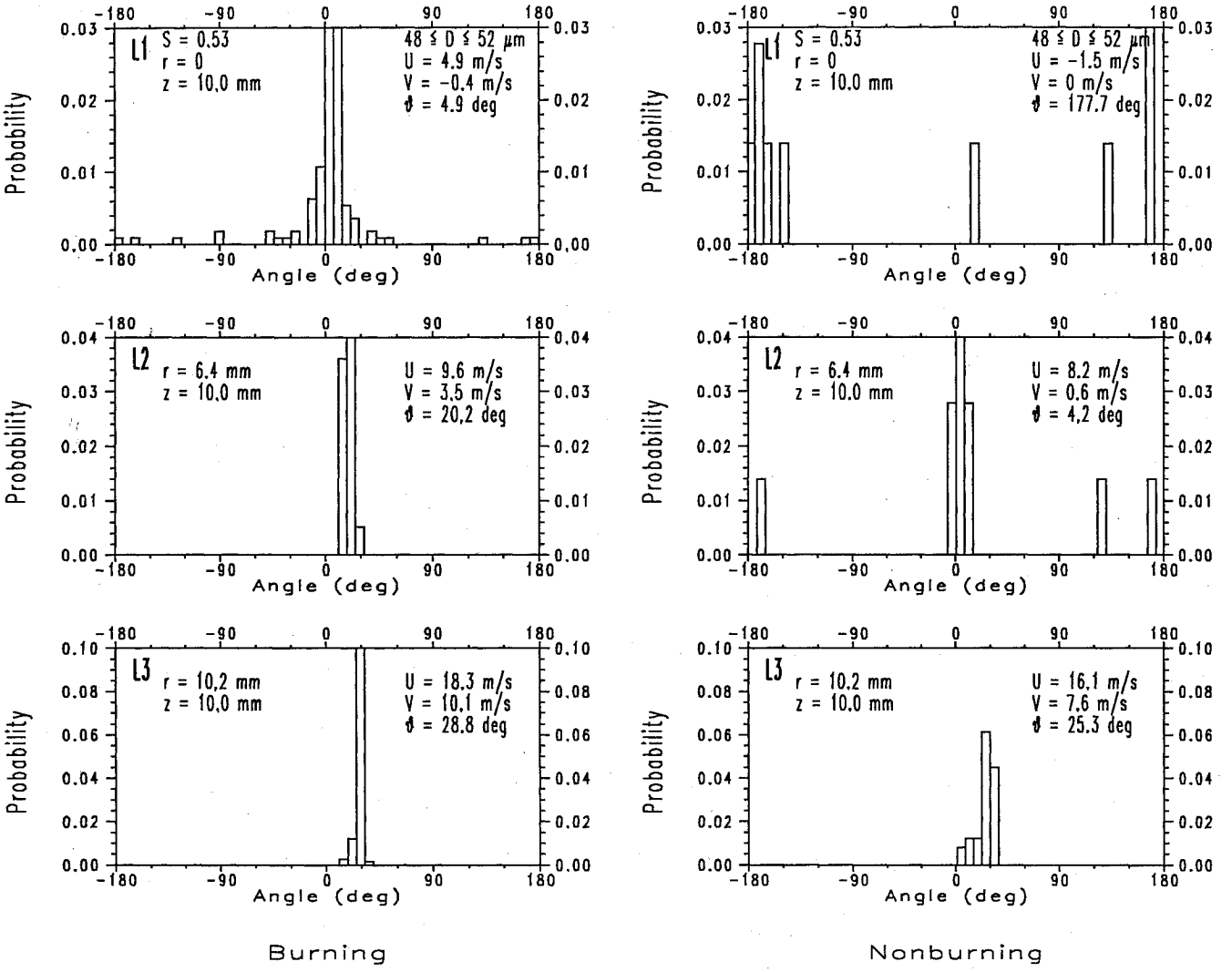

Fig. 14 Probability distributions for droplet trajectory angles at three different locations (L1–L3) in the burning and nonburning sprays for droplets in the size range of 48–52 μm.

conditions of the spray examined here the droplet tangential velocity component decays rapidly within a few millimeters downstream of the nozzle and is essentially negligible.[4] Therefore, the axial and radial velocity components alone determine the direction of droplet motion in the two-dimensional (z–r) plane, where $\theta = \tan^{-1}(v/u)$.

Variation of the droplet mean angle is presented in Fig. 11 at the various aforementioned locations within both the burning and nonburning sprays. In the outer radial regions of the spray, there is little difference in the direction of droplet motion between the burning and nonburning sprays, with the mean direction of droplet motion being in the nominal direction of the spray cone half-angle (see Fig. 8), which is about 30 deg. However, near the spray centerline and upstream close to the nozzle, droplets in the burning spray are moving in directions opposite to those in the nonburning spray (as a result of significant droplet recirculation in the nonburning spray). For example, in the burning spray $\theta \approx 0$ at the axis of the burner for $z = 10$ and 25.4 mm, while for the nonburning spray $\theta \approx 180$ deg. Reasons for these differences in mean direction near the center of the spray are explored further by examining the distributions of droplet angle.

Distributions of droplet angle are presented in Figs. 12–14 at positions L1 ($r = 0$), L2 ($r = 6.4$ mm), and L3 ($r = 10.2$ mm), from the centerline of the spray ($\Delta = 0$) to the spray boundary, at $z = 10$ mm for both the burning and nonburning sprays. At L4 and L5 too few droplets existed to construct meaningful histograms. The results presented in Fig. 12 show the distributions for all size classes, whereas the data in Figs. 13 and 14 are for specified size ranges: $1 < D < 5$ μm (hereafter referred to as 3-μm size droplets) for Fig. 13, and $48 < D < 52$ μm (referred to as 50-μm size droplets) for Fig. 14.

Differences between burning and nonburning conditions are evident from Fig. 12. In the nonburning case, there is a wide distribution of angles at locations L1 and L2, which becomes narrower towards the spray boundary at L3. The wide distributions at locations L1 and L2 indicate the presence of two counterflowing streams, namely, droplets originating from the nozzle (angle = ±90 deg) and recirculated droplets (±90 < angle < ±180 deg). In the burning spray, most droplets are moving downstream away from the nozzle, while in the nonburning spray most droplets are moving upstream toward the nozzle at L1, and to a lesser extent at L2. It is worth noting that there are still droplets moving upstream in the burning spray (e.g., note L1). The upstream motion of droplets shown in Fig. 12 is indicative of the effect of combustion gas recirculation on droplet motion. Since the swirl number is the same for both the burning and nonburning sprays, it is evident that droplet transport is less effected by swirling gases in the burning spray, and therefore, droplets tend to move in a ballistic fashion. It is interesting to note the similarity of the burning case to the nonburning case for $S = 0$, in that the expectation is also for ballistic transport of droplets (as evidenced by laser sheet visualization of droplet trajectories in similar sprays[3,4]).

Precisely how combustion affects droplet trajectories is a matter of speculation. The drag force F_D on a droplet can

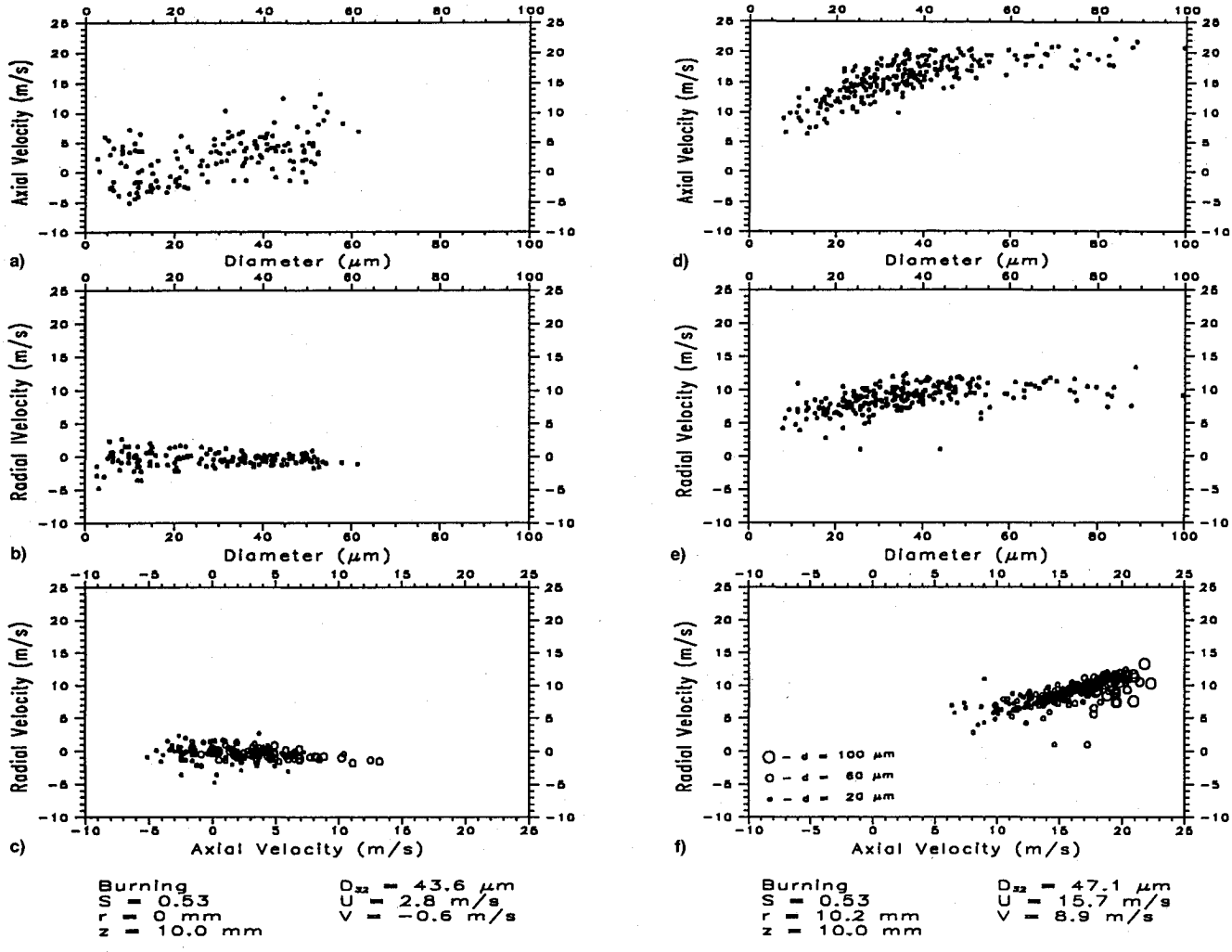

Fig. 15 Axial velocity/diameter, radial velocity/diameter, and axial/radial velocity correlations, respectively, at the centerline (location L1, frames a–c) and spray boundary (location L3 frames d–f) for the burning spray with $S = 0.53$. Axial/radial velocity correlations are coded to represent the change in droplet diameter.

be expressed in terms of gas phase properties as $F_D \approx C(D\bar{V}_{rel})^{2-n}\mu^n\rho^{1-n}$. The term C is a proportionality constant for a drag coefficient that is inversely proportional to the Reynolds number raised to a power n, where typically[17] $0 < n < 1$. As conditions are changed to reduce the droplet relative velocity, and/or gas phase viscosity and density, the term F_D should decrease for droplets of given diameter. Under such conditions, droplets would tend to move ballistically. As shown in Fig. 11, this is more prevalent for droplets in a burning spray than in a nonburning spray along the axis of the burner. Differences in gas temperatures between a burning and nonburning spray can create substantial differences in properties that would effect the drag force. For example, since $\rho \sim 1/T$ and $\mu \sim T^{1/2}$ (from kinetic theory), then $F_D \sim \bar{V}_{rel}^{2-n}T^{3/2n-1}$. Depending on the value of n, the drag force can increase or decrease as temperature increases for a given relative velocity and droplet size. For $n < 2/3$, the drag force will decrease as temperature increases, but such a range for n would require comparatively larger Reynolds numbers (typically greater than 1×10^2 (Ref. 17) than are likely to be present for droplets in the spray. A more applicable situation is $n > \frac{2}{3}$, in which case the term F_D will increase as temperature increases, and thereby result in less ballistic transport of droplets. However, the opposite is observed in these sprays, as shown by the size-classified angle distributions of Figs. 13 and 14, where significant numbers of droplets are moving upstream in the nonburning spray and the gas temperatures are comparatively lower. Evidently, the relative velocity (not measured as discussed previously) between droplets and surrounding gas must be lower in the burning spray (because of the effect of the high-temperature gases on the gas-phase flowfield), to compensate for the temperature dependence of physical properties on droplet drag.

The size-classified angle distributions shown in Figs. 13 and 14 provide a more detailed picture of individual droplet transport. Figure 13 shows that while the 3-μm-class droplets are generally moving in the downstream direction along the centerline (see frame L1) for the burning spray ($\theta = 27.1$ deg), the range of directions is comparatively wide. By contrast, in the lower-temperature nonburning spray a significant number of 3-μm droplets are moving upstream at locations L1 and L2. This trend reflects the stronger effect of recirculating gas phase motion on droplet relative velocity and drag than the thermal effect, which would tend to decrease droplet drag. It should be noted, however, that there are some 3-μm droplets at location L1 that are moving in the downstream direction, which reflects the statistical variation in droplet velocity. At location L3 (close to the spray boundary) the few 3-μm size droplets that could be detected are moving in the downstream direction for both the burning and nonburning sprays.

It is expected that smaller droplets will typically be carried along with the surrounding flowfield. Transport of larger droplets is expected to be relatively unaffected by the gas-phase flow pattern. As shown in Fig. 14, 50-μm size droplets in the burning spray have a relatively narrow distribution of angles with only a few droplets deviating from the mean direction. At location L1 the mean direction of droplet motion is small

(5.2 deg). Closer to the spray boundary (at locations L2 and L3) the mean direction of droplet motion increases, from 20.1 deg at $r = 6.4$ mm to 28.9 deg at $r = 10.2$ mm, which would be consistent with the hollow-cone nature of the spray. Also, virtually no 50-μm size droplets are moving in upstream directions at locations L2 and L3.

For the nonburning spray, some 50-μm droplets are moving upstream as illustrated in Fig. 14 at locations L1 and L2. Such upstream motion of large droplets is surprising as it shows the comparatively strong entrainment of droplets by the surrounding air for the nonburning spray. Close to the spray boundary (at location L3) virtually all of the 50-μm droplets are moving in the direction of the nominal spray cone angle with no upstream droplet motion suggested by the data.

C. Velocity and Droplet Size Correlation

The correlation among the droplet diameter and velocity components provides additional information for understanding mechanisms of droplet transport in sprays. Figure 15 shows such correlations at locations L1 and L3 under burning conditions. Data under nonburning conditions are not presented because of the similarities to the burning case and have been reported previously.[5] The symbols in frames c and f are coded to the droplet size as shown in the inset of Fig. 15f.

At location L1 (burner centerline), the axial droplet velocity component is weakly correlated with diameter (i.e., weak linear dependence between diameter and axial velocity with a correlation coefficient r^2 of 0.5) as shown in Fig. 15a, though there is a slight increase in the value of u as diameter increases. Furthermore, for any given diameter, the axial velocity varies over a relatively large range. For example, the axial velocity of 10-mm-diam droplets varies between about -5 to 7 m/s as shown in Fig. 15a. By contrast, the radial velocity component is much smaller and shows much less scatter for a given droplet diameter than the axial component as shown in Fig. 15b. Figure 15c shows the correlation between the two velocity components at location L1. The axial component is weakly dependent on the radial component, which is close to zero as shown in Fig. 15c. In terms of θ, the data in Fig. 15c are consistent with a mean direction of droplet motion that is essentially along the centerline of the burner ($\theta = 12.1$ deg as shown in Fig. 12) because of the small radial velocity component. The size-coded symbols in Fig. 15c show the tendency of larger droplets to have larger axial velocity components than smaller droplets.

At location L3 (near the spray boundary, see Figs. 15d and 15e) the results show different trends than along the spray centerline. Whereas the axial velocity component does not vary strongly with droplet diameter at location L1 (see Fig. 15a), the correlation between axial velocity and diameter is more pronounced at location L3 ($r^2 \approx 0.75$) where the value of u increases as diameter increases over the range $5 < D < 60$ μm. For $D > 60$ μm, the correlation appears to approach a constant value. In this range, the radial velocity component increases at a slower rate and also appears to approach an asymptotic value for larger droplet diameters. Near the spray boundary, where the droplets are moving at a comparatively higher velocity, a simple force balance on droplets shows that droplet deceleration is inversely proportional to diameter squared.[18] Since larger droplets will decelerate less than smaller droplets, the velocity of larger droplets is expected to be less influenced by droplet diameter than smaller droplets (because of the $1/D^2$ dependence of droplet deceleration). For larger droplets that would experience minimal deceleration, the droplet velocity should be independent of diameter in the spray. This is consistent with the trends shown in Figs. 15d and 15e.

The correlation between velocity components near the spray boundary, shown in Fig. 15f, is consistent with the direction of motion shown in Fig. 12. The slope of the best fit line drawn through the size-classified data is the tangent of the trajectory angle, which at location L3 in Fig. 15f is approximately 12 deg, as shown in Figs. 11 and 12. However, it is evident from Fig. 12 that there is a range of angles associated with the velocity components as reflected by the distribution of angles shown in Fig. 12.

IV. Summary

Droplet transport was examined in a kerosene spray flame using a phase Doppler size and velocity system. The effects of combustion were studied by comparing a burning spray to that of one under nonburning conditions for the same operating conditions. The results from this investigation were the following:

1) Mean properties are adequate for describing global features of the spray near the spray boundary, but significant deviations from the mean can occur near the centerline where some droplets are moving in directions opposite from the mean.

2) Near the spray centerline, droplet recirculation is reduced significantly under burning conditions. Consequently, droplets are not transported upstream as readily as in the nonburning spray. However, some droplet transport still occurs in the upstream direction, opposite to that of the mean flow. Unexpectedly, some larger size droplets are also found to be entrained in the recirculation pattern in addition to the smaller ones. On the spray boundary, however, few droplets deviate from the mean direction.

3) Near the spray boundary, droplet velocity increases as droplet diameter increases, and appears to reach an asymptotic value where droplet velocity is independent of diameter.

4) Combustion appears to retard the influence of the surrounding gas flowfield on droplet trajectories. Thus, larger droplets tend to move downstream ballistically (away from the nozzle). This observation suggests that the drag on droplets in the burning spray is lower than in the nonburning spray. It is speculated that this is because of a lowering of the relative velocity between the droplet and surrounding gas under burning conditions.

Acknowledgments

The contributions of CTA were supported by the New York State Center for Hazardous Waste Management, A. Scott Weber, Director. The technical assistance of Michael J. Carrier and James D. Allen is greatly appreciated.

References

[1]Hillmanns, R., Lenze, B., and Leuckel, W., "Flame Stabilization and Turbulent Exchange in Strongly Swirling Natural Gas Flames," *21st International Symposium on Combustion*, The Combustion Inst., Pittsburgh, PA, 1986, pp. 1445–1453.

[2]Goix, P. J., Edwards, C. F., Cessou, A., Dunsky, C. M., and Stepowski, D., "Structure of a Methanol/Air Coaxial Reacting Spray Near the Stabilization Region," *Combustion and Flame*, Vol. 98, 1994, pp. 205–219.

[3]Presser, C., Gupta, A. K., Semerjian, H. G., and Avedisian, C. T., "Droplet Transport in a Swirl-Stabilized Spray Flame," *Journal of Propulsion and Power*, Vol. 10, No. 5, 1994, pp. 631–638.

[4]Presser, C., Gupta, A. K., and Semerjian, H. G., "Aerodynamic Characteristics of Swirling Spray Flames: Pressure-Jet Atomizer," *Combustion and Flame*, Vol. 92, Nos. 1/2, 1993, pp. 25–44.

[5]Presser, C., and Gupta, A. K., "Behavior of Droplets in Pressure-Atomized Fuel Sprays with Coflowing Air Swirl," *Heat Transfer in Fire and Combustion Systems*, edited by B. Farouk, M. P. Menguc, R. Viskanta, C. Presser, and S. Chellaiah, HTD-Vol. 250, American Society of Mechanical Engineers, New York, 1993, pp. 79–92.

[6]Presser, C., and Gupta, A. K., "Behavior of Droplets in Pressure-Atomized Fuel Sprays," AIAA Paper 93-0132, Jan. 1993.

[7]Gupta, A. K., Lilley, D. G., and Syred, N., *Swirl Flows*, Abacus Press, Kent, England, UK, 1984.

[8]Bachalo, W. D., and Houser, M. J., "Phase/Doppler Spray Analyzer for Simultaneous Measurements of Drop Size and Velocity Distributions," *Optical Engineering*, Vol. 23, No. 5, 1984, pp. 583–590.

[9]Sankar, S. V., Buermann, D. H., and Bachalo, W. D., "Nonintrusive Characterization of Liquid-Liquid Mixing in Sprays," AIAA Paper 95-0138, Jan. 1995.

[10]Schaub, S. A., Alexander, D. R., and Barton, D. R., "Theoretical Analysis of the Effects of Particle Trajectory and Structural Resonances on the Performance of a Phase-Doppler Particle Analyzer," *Applied Optics*, Vol. 33, No. 3, 1994, pp. 473–483.

[11]Gréhan, G., Gouesbet, G., Naqwi, A., and Durst, F., "Trajectory Ambiguities in Phase Doppler Systems: Study of a Near-Forward and a Near-Backward Geometry," *Particle and Particle System Characterisation*, Vol. 11, 1994, pp. 133–144.

[12]Hodges, J. T., Presser, C., Gupta, A. K., and Avedisian, C. T., "Analysis of Droplet Arrival Statistics in a Pressure-Atomized Spray Flame," *25th International Symposium on Combustion*, The Combustion Inst., Pittsburgh, PA, 1995, pp. 353–361.

[13]Zhu, J. Y., Rudoff, R. C., Bachalo, E. J., and Bachalo, W. D., "Number Density and Mass Flux Measurements Using the Phase Doppler Particle Analyzer in Reacting and Nonreacting Swirling Flow," AIAA Paper 93-0361, Jan. 1993.

[14]Bulzan, D. L., "Velocity and Drop Size Measurements in a Swirl-Stabilized, Combusting Spray," *SPIE-The International Society for Optical Engineering*, edited by L. C. Liou, Vol. 1862, 1993, pp. 113–122.

[15]McDonell, V. G., and Samuelsen, G. S., "Application of Laser Interferometry to the Study of Droplet/Gas Phase Interaction and Behavior in Liquid Spray Combustion Systems," *Combustion Science and Technology*, Vol. 74, Nos. 1–6, 1990, pp. 343–359.

[16]Edwards, C. F., and Rudoff, R. C., "Structure of a Swirl-Stabilized Spray Flame by Imaging, Laser Doppler Velocimetry, and Phase Doppler Anemometry," *23rd International Symposium on Combustion*, The Combustion Inst., Pittsburgh, PA, 1990, pp. 1353–1359.

[17]Lefebvre, A. H., *Atomization and Sprays*, Hemisphere, New York, 1989, pp. 301–305.

[18]Presser, C., Gupta, A. K., Hodges, J. T., and Avedisian, C. T., "Interpretation of Size-Classified Droplet Velocity Data in Swirling Spray Flames," AIAA Paper 95-0283, Jan. 1995.